

## Supplemental Information

### A Single T Cell Receptor Bound to Major

### Histocompatibility Complex Class I and Class II

### Glycoproteins Reveals Switchable TCR Conformers

Lei Yin, Eric Huseby, James Scott-Browne, Kira Rubtsova, Clamencia Pinilla, Frances Crawford, Philippa Marrack, Shaodong Dai, and John W. Kappler

#### Supplemental Data Inventory

##### **There are three supplemental Figures.**

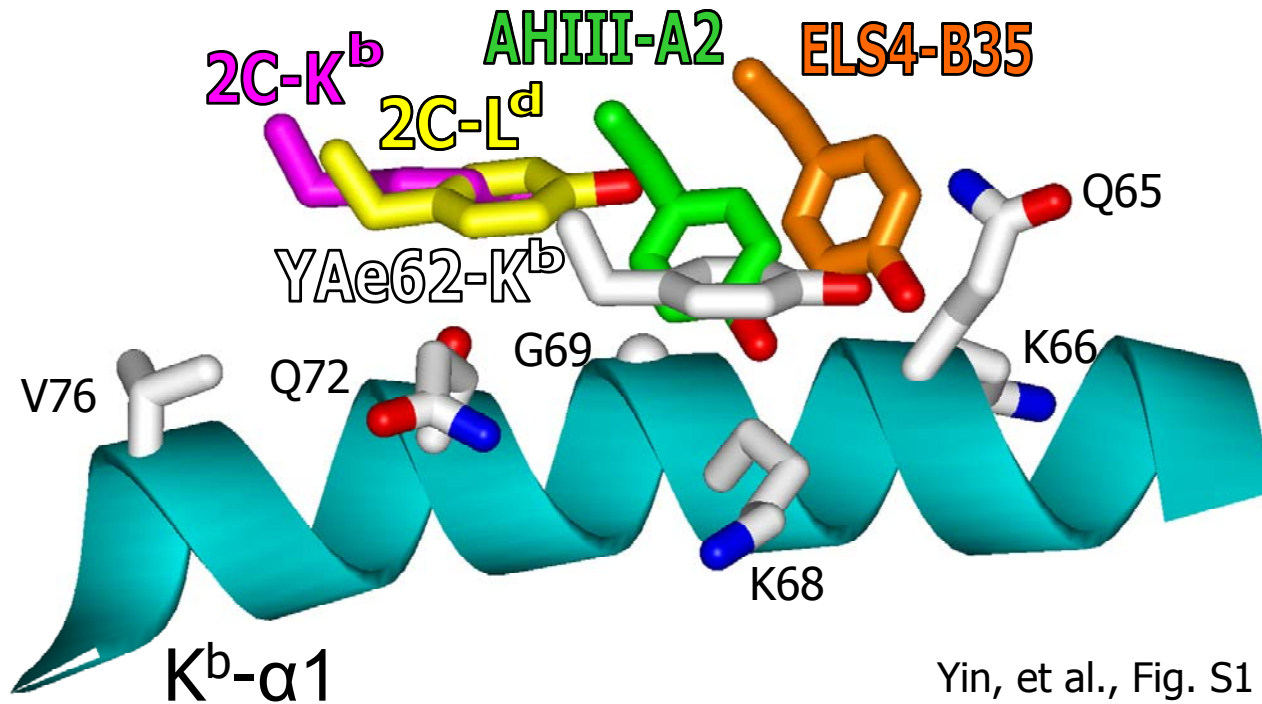
1. Figure S1 extends the data in Figure 3b(right panel). It compares the position of the YAE62 V $\beta$  Y48 on the Kb  $\alpha$ 1  $\alpha$  helix to its position in other structures involving TCRs with mouse V $\beta$ 8-like V $\beta$ s bound to MHC I ligands.
2. Figure S2 extends the data in Figure 4. It shows the effect of mutating YAE62 V $\beta$  CDR amino acids other than CDR2 Y46, Y48, and E54 on the recognition of IA<sup>b</sup>-p3K and K<sup>b</sup>-pWM.
3. Figure S3 is related to Figure 6. Panel A shows sample electron density confirming the separation of the  $\beta$ -strands that support V $\alpha$  CDR3 when the YAE62 TCR binds to Kb-pWM. Panels B and C show the comparison of over 3 dozen overlaid V $\alpha$  and V $\beta$  domains that identified human V $\alpha$ 4 and mouse V $\beta$ 2 containing TCRs as examples of those with disrupted V to J  $\beta$ -strands.

**There are two supplemental Tables.**

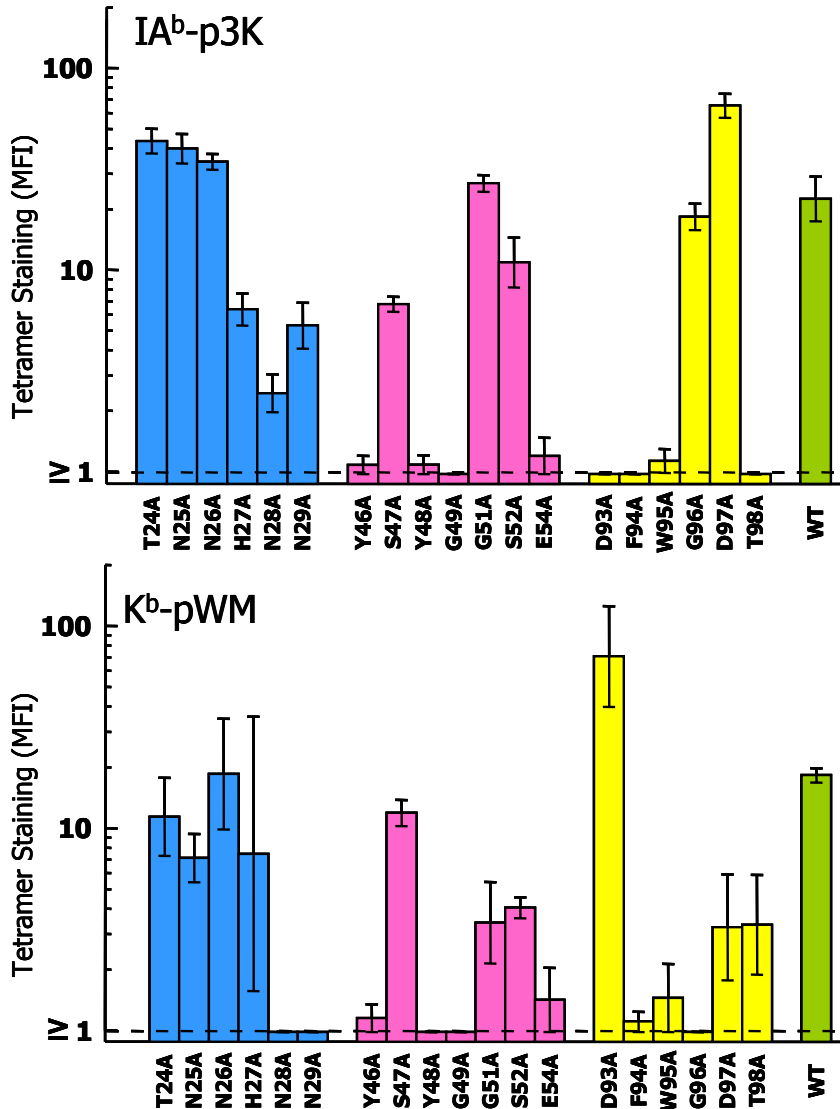
Table S1 is related to Figure 2 and show all of the data collection and refinement statistics for the x-ray diffraction data and structural model of YAc62 bound to K<sup>b</sup>-pWM.

Table S2 (Excel Spreadsheet available online) shows the full atom-to-atom contact data for the YAc62 TCR bound to K<sup>b</sup>-pWM that is summarized in Table 1.

**There are Supplemental Experimental Procedures**

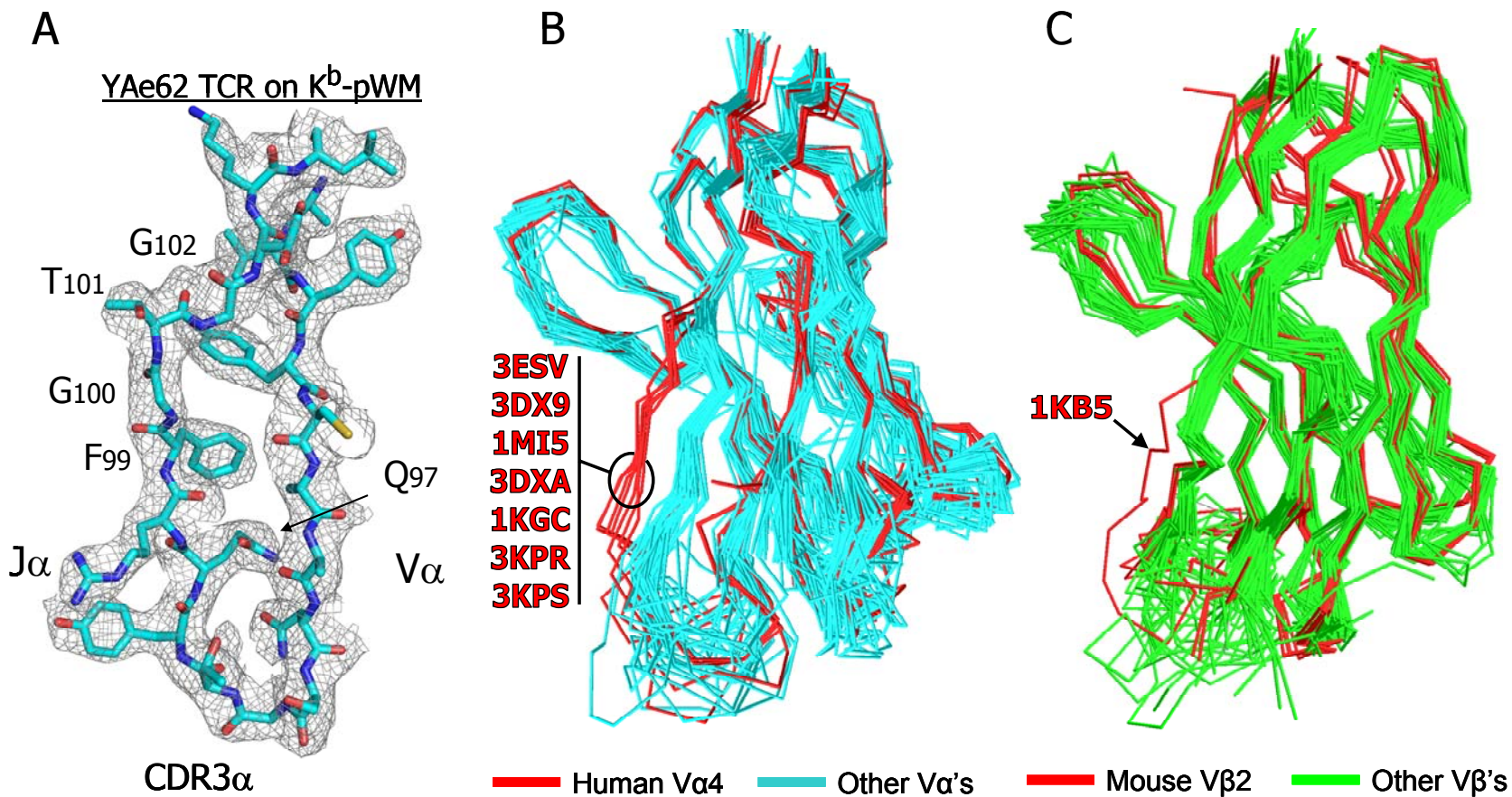


**Figure S1** (Related to Fig.3)– The extended range of TCR  $\beta$ Y48 interaction with MHC I ligands. A portion of the  $\alpha$ 1 helix of  $K^b$  in the YAe62/ $K^b$ -pWM complex is shown as a ribbon (cyan) with wireframe representation of six  $K^b$  amino acid side chains (CPK coloring). A wireframe representation of the side chain of YAe62  $\beta$ Y48 is also shown. To show the relative position of  $\beta$ Y48 in four other TCR/MHCI structures bearing  $V\beta$  elements with Y48, these structures were overlaid with the  $K^b$ -pWM using the 8 core  $\alpha$ 1/ $\alpha$ 2  $\beta$ -strands and the  $\alpha$ 1 helix. For each structure the side chain of  $\beta$ Y48 is shown (PDB-2CKB, magenta, 2C bound to  $K^b$ ; PDB-2OI9, yellow, 2C bound to  $L^d$ ; PDB-1LP9, green, AHIII bound to HLA-A2; PDB-2NX5, orange, ELS4 bound to HLA-B35, PDB-2NX5).



Yin, et al., Fig. S2

**Figure S2** (Related to Fig. 4) – Effect of V $\beta$  mutations on the binding of the YAe62 TCR to IA<sup>b</sup>-p3K and K<sup>b</sup>-pWM. A TCR<sup>-</sup> hybridoma was retrovirally transduced with wt YAe62  $\alpha$  chain and subsequently retrovirally transduced with wt YA62  $\beta$  chain or with  $\beta$  chains bearing alanine substitutions within the V $\beta$  CDR loops. The resultant transductants were analyzed by flowcytometry with fluorescent tetramers of IA<sup>b</sup>-p3K or K<sup>b</sup>-pWM, costaining with a fluorescent anti-C $\beta$  MAb. The tetramer mean fluorescence intensity for cells bearing equivalent surface TCR levels is shown (average and SEM of three experiments).



Yin, et al., Fig. S3

**Figure S3** – (Related to Fig. 6 ) A. Sample electron density for the YAe62/K<sup>b</sup>-pWM complex. The V<sub>α</sub> CDR3 loop and two associated β strands are shown for the YAe62 TCR bound to K<sup>b</sup>-pWM as wireframe. The associated electron density (2Fo-Fc) is shown at 1σ in grey. The loss of the usual H-bonding between the backbone of the β stands. the gain of H-bonding to a αQ97 and the position of

the FGXG motif are clearly seen in the density. B & C. Over three dozen structures obtained from the PDB containing free V $\beta$  domains, free V $\alpha$  domains, free complete TCRs and TCRs bound to either MHC I or MHC II ligands were overlaid by either V $\alpha$  (B) or V $\beta$  (C). The overlaid V domains are shown as C $\alpha$  traces. The V $\alpha$  domains are cyan except for those containing human V $\alpha$ 4 which are red. The V $\beta$  domains are green except for those containing mouse V $\beta$ 2, which are red. V $\alpha$  PDB Nos: 1A07, 1BD2, 1D9K, 1FO0, 1G6R, 1J8H, 1KJ2, 1LP9, 1MI5, 1MWA, 1NFD, 1U3H, 1YMM, 1ZGL, 2AK4, 2BNQ, 2CDF, 2CDG, 2ESV, 2IAM, 2NX5, 2PXY, 3C5Z, 3C60, 3C6L, 3DXA, 3FFC, 3HUJ, 3MBE, 3MFF, 3MV7, 1AC6, 1H5B, 1KGC, 2Q86, 2Z31, 2Z35, 3DX9, 3GSN, 3KPR, 3KPS. V $\beta$  PDB Nos.: 1A07, 1BD2, 1D9K, 1FO0, 1G6R, 1J8H, 1KJ2, 1LP9, 1MI5, 1MWA, 1NFD, 1U3H, 1YMM, 1ZGL, 2AK4, 2BNQ, 2CDF, 2CDG, 2ESV, 2IAM, 2NX5, 2PXY, 3C5Z, 3C60, 3C6L, 3DXA, 3FFC, 3HUJ, 3MBE, 3MFF, 3MV7, 1FYT, 1KB5, 1NAM, 1OGA, 2AXH, 2CDE, 2OL3, 2PO6, 3HE7.

Table S1 (Related to Figure 2) – Diffraction data collection and refinement statistics

Space group	I222 <sup>a</sup>	P3(2)21 <sup>a</sup>
<b>Data Collection</b>		
Cell dimensions <i>a, b, c</i> (Å)	118.9, 146.4, 168.6	69.1, 69.1, 409.4
Resolution (Å)	20-2.90 (3.0-2.9)	50-3.4 (3.36-3.3)
Rmerge (%)	10.9 (53.1)	15.9 (99.0)
I/s (I)	7.1 (2.0)	12.8 (1.4)
Completeness (%)	96.9 (91.1)	99.3 (99.8)
Redundancy	3.8 (2.6)	4.4 (5.0)
<b>Refinement</b>		
Resolution (Å)	20.0-2.9 (3.00-2.90)	50.0-3.4 (3.38-3.30)
No. reflections	30372 (2416)	17196 (1184)
Complexes per A.U.	1	1
Rwork/Rfree	20.2/25.4 (33.7/42.5)	30.2/38.2 (41.4/41.9)
No. of atoms		
Protein	6592	
Water	0	
B-factors		
TCR V domains	46.0	
TCR C domains	69.1	
MHC-peptide	60.2	
H <sub>2</sub> O	N/A	
R.m.s deviations		
Bond lengths (Å)	0.010	
Bond angles (°)	1.348	
Ramachandran plot		
Most favored region (%)	85.5%	
Additional allowed region (%)	14.1%	
Generously allowed region (%)	0.4%	
Disallowed region (%)	0%	

<sup>a</sup>Outer shell

## **Supplemental Experimental Procedures**

### **T cell assays and identification of peptide mimotopes**

$10^5$  CD8<sup>+</sup> YAe62 TCR transgenic T cells were incubated for 48 hours in round bottomed wells with  $5 \times 10^5$  MHCII- Ii- mitomycin treated spleen cells that had been prepulsed with varying doses of the TPI 921 library (Pinilla et al., 1992) or purified individual peptides. For the last 12 hours of the incubation 3H-thymidine was added to the cultures. Thymidine incorporation in control wells, in which the spleen cells had not been pulsed with peptide, was subtracted from the results. To deconvolute information from the library experiments, we screened a second set of semi-purified synthesized peptides containing various combinations of the potential amino acid at each position. Six of these peptides induce significant proliferation of YAe62 CD8<sup>+</sup> T cells. These peptides were re-synthesized, purified, retested and failed to activate YAe62 T cells. To identify the active peptide in the semi-purified 9mer peptides, the peptides were analyzed by mass spectrometry at the National Jewish Molecular Resource Center. An identical WIYVYRPM 8mer peptide was identified within each of the active 9mer semi-purified peptide preps. The activity of this 8mer peptide, referred to as pWM, was confirmed with a re-synthesized purified preparation tested as above.

Cytotoxicity experiments were done by activating  $2 \times 10^7$  spleen cells from YAe62 Tg MHCII<sup>-</sup> mice with  $3 \times 10^7$  Mitomycin C treated C57BL/6 spleen cells pre-incubated with 0.1ug/ml 3K peptide in 10 ml cultures for 6 days. At that time the activated YAe62 CD8 T cells were assayed for their ability to lyse 3T3 target cells which had or had not been transduced to express K<sup>b</sup>, or D<sup>b</sup> and which had or had not been pulsed with or without 5ug/ml of pWM. Cells expressing IA<sup>b</sup>-p3K were used as a positive control target.. Cytotoxicity assays were done using standard techniques (Huseby et al., 1999). Briefly, target cells were labeled by incubation with 100  $\mu$ Ci of (<sup>51</sup>Cr)O<sub>4</sub> (Amersham, Arlington Heights, IL) for 60 min, washed, and incubated with effector cells in a standard 4-h <sup>51</sup>Cr release assay. The percent lysis was calculated as (<sup>51</sup>Cr release in the presence of CTLs – spontaneous <sup>51</sup>Cr release) x 100/(total <sup>51</sup>Cr release in 2% Nonidet P-40 – spontaneous <sup>51</sup>Cr release).

### **Surface Plasmon Resonance**

TCR/MHC interactions were assessed by surface plasmon resonance (SPR) using a BIAcore 2000 instrument and a streptavidin BIA sensor chip. Biotinylated IA<sup>b</sup>-p3K, K<sup>b</sup>-



pWM and K<sup>b</sup>-pOVA molecules were captured (~3000 RU) in three of the sensor flowcells. The human MHCII molecule, HLA-DR52c was immobilized in a fourth control flowcell. Various concentrations of soluble YAE62 TCR were injected sequentially through the four flowcells for 30 sec and the SPR signal recorded. To correct the data for the fluid phase SPR signal, for each concentration of the TCR, the four binding curves were aligned using BIAcore software and the SPR signal obtained with HLA-DR52c subtracted from the other three curves. The corrected equilibrium data for IAb-p3K and K<sup>b</sup>-pWM were used to construct a Scatchard plot. The K<sub>D</sub> values (μM) for the two ligands were calculated as -1/slope of the least squares regression line fit to the data.

### **Protein Expression and purification**

The DNA encoding K<sup>b</sup> (extracellular domains) and β2m covalently attached to pWM were cloned into a single baculovirus as previously described (White et al., 1999). The genes were mutated to introduce cysteines into K<sup>b</sup> replacing tyrosine 84 and into the linker that attaches β2m to pWM replacing a glycine at position 2 (Lybarger et al., 2003). The soluble, disulfide linked K<sup>b</sup>-pWM complex in the supernatant of virus infected HighFive insect cells was purified by immunoaffinity chromatography using an anti-β2m monoclonal antibody followed by size exclusion chromatography using a Superdex-200. For BIAcore experiments soluble YAE62 TCR was expressed in baculovirus as previously described (Huseby et al., 2005). For crystallography, as previously described (Dai et al., 2008; Tynan et al., 2007), the V<sub>α</sub> and V<sub>β</sub> portions of the YAE62 TCR were produced fused to the extracellular portions of human C<sub>α</sub> and C<sub>β</sub>, respectively, in E. coli inclusion bodies. They were solubilized, mixed and refolded to produce the complete YAE62 TCR .

### **Crystal Production and Data Collection**

An equimolar mixture of YAE62 TCR and K<sup>b</sup>-pWM was crystallized by mixing 0.5 ul of complex solution at a concentration of 15mg/ml with an equal volume of reservoir solution. The complex crystallized in two different space groups: one with spacegroup, I222, was crystallized in 17% PEG3350, 100mM sodium malonate pH7.0 and the other with another space group, P3(2)21, was crystallized in 17% PEG3350, 5% glycerol, 100mM sodium succinate, pH7.0.

X-ray diffraction data were collected at the Advanced Light Source on beam line 8.2.2 under liquid-nitrogen cryo-conditions at 100°K. Both crystals were flash-cooled in liquid nitrogen after a flash-soak in a cryoprotection solution consisting of the reservoir solution with additional concentration of glycerol (25%). The data were indexed, integrated, scaled and merged using HKL2000.

### **Structure Determination**

The structures of YAE-K<sup>b</sup>-pWM complex in both crystals were determined by molecular replacement using Phaser with the YAE62 TCR(PDB 3C60) and K<sup>b</sup>-pEV8 (PDB 2CKB) as search models, respectively. After an initial round of rigid-body refinement, the models were inspected and manually fitted with program Coot. The models were then subjected to several rounds of alternating simulated annealing/positional refinement in Phenix followed by B factor refinement in Phenix. Model building was performed using program Coot. Simulated annealing omit maps were routinely used to remove the model bias. All models have good stereochemistry, as determined by program Procheck.

### **Structure analysis**

Buried molecular surface areas were calculated using GRASP. NCONT in CCP4 was used to analyze the contacts between the TCRs and their ligands. Atoms within 4.5Å of each other were considered part of the interface. Contacts involving potential electron donors and acceptors (O or N) within 3.5Å were considered potential hydrogen bonds or salt bridges. Other contacts were considered van der Waals contacts. Molecular superimpositions and figures were created with pymol and Swiss PDB Viewer(Ver4.0).

### **TCR mutational analysis**

Wild-type and indicated Ala-substitution mutants of YAE-62.8 V $\alpha$  and V $\beta$  were cloned in MSCV-based retroviral plasmids with an internal ribosomal entry site plus either green fluorescent protein or human nerve growth factor receptor as a reporter. TCR chains were expressed in a TCR-deficient hybridoma line (5KC-73.8.20) by retroviral transduction, as described previously (Rubtsova et al., 2009). Cells expressing equivalent levels of TCR and CD4 were isolated by flow cytometry cell sorting.

For tetramer staining, hybridomas were incubated with 20ug/ml phycoerythrin-labeled IA<sup>b</sup>-p3K or K<sup>b</sup>-pWM tetramers for 90 minutes at 37°C in the presence of the anti-CD16/CD32 Mab, 2.4G2. At this time, allophycocyanin-labeled anti-C $\beta$  (clone H57-597) was added and incubated for an additional 20 minutes at 25°C. Cells were analyzed by flow cytometry on an LSRII instrument (BD Biosciences, San Diego, CA) and data were analyzed in FlowJo software (Treestar, Ashland, OR). For quantitation, the amount of tetramer bound to cells expressing the same level of C $\beta$  were compared.

## Supplemental References

- Dai, S., Huseby, E.S., Rubtsova, K., Scott-Browne, J., Crawford, F., Macdonald, W.A., Marrack, P., and Kappler, J.W. (2008). Crossreactive T Cells spotlight the germline rules for alphabeta T cell-receptor interactions with MHC molecules. *Immunity* *28*, 324-334.
- Huseby, E.S., Ohlen, C., and Goverman, J. (1999). Cutting edge: myelin basic protein-specific cytotoxic T cell tolerance is maintained in vivo by a single dominant epitope in H-2k mice. *J Immunol* *163*, 1115-1118.
- Huseby, E.S., White, J., Crawford, F., Vass, T., Becker, D., Pinilla, C., Marrack, P., and Kappler, J.W. (2005). How the T cell repertoire becomes peptide and MHC specific. *Cell* *122*, 247-260.
- Lybarger, L., Yu, Y.Y., Miley, M.J., Fremont, D.H., Myers, N., Primeau, T., Truscott, S.M., Connolly, J.M., and Hansen, T.H. (2003). Enhanced immune presentation of a single-chain major histocompatibility complex class I molecule engineered to optimize linkage of a C-terminally extended peptide. *J Biol Chem* *278*, 27105-27111.
- Pinilla, C., Appel, J.R., Blanc, P., and Houghten, R.A. (1992). Rapid identification of high affinity peptide ligands using positional scanning synthetic peptide combinatorial libraries. *Biotechniques* *13*, 901-905.
- Rubtsova, K., Scott-Browne, J.P., Crawford, F., Dai, S., Marrack, P., and Kappler, J.W. (2009). Many different Vbeta CDR3s can reveal the inherent MHC reactivity of germline-encoded TCR V regions. *Proc Natl Acad Sci U S A* *106*, 7951-7956.
- Tynan, F.E., Reid, H.H., Kjer-Nielsen, L., Miles, J.J., Wilce, M.C., Kostenko, L., Borg, N.A., Williamson, N.A., Beddoe, T., Purcell, A.W., *et al.* (2007). A T cell receptor flattens a bulged antigenic peptide presented by a major histocompatibility complex class I molecule. *Nat Immunol* *8*, 268-276.
- White, J., Crawford, F., Fremont, D., Marrack, P., and Kappler, J. (1999). Soluble class I MHC with beta2-microglobulin covalently linked peptides: specific binding to a T cell hybridoma. *J Immunol* *162*, 2671-2676.